Improving breast cancer outcome by preoperative systemic therapy and image-guided surgery

Mieog, J.S.D.

Citation

Mieog, J. S. D. (2011, October 26). *Improving breast cancer outcome by preoperative systemic therapy and image-guided surgery*. Retrieved from https://hdl.handle.net/1887/17983

Part IIB

Sentinel lymph node mapping

Chapter 11

Towards optimization of imaging system and lymphatic tracer for near-infrared fluorescent sentinel lymph node mapping in breast cancer

Mieog JSD[1], Troyan SL[1], Hutteman M[1], Donohue KJ, van der Vorst JR, Stockdale A, Liefers GJ, Choi HS, Gibbs-Strauss SL, Putter H, Gioux S, Kuppen PJK, Ashitate Y, Löwik CWGM, Smit VTHBM, Oketokoun R, Ngo LH, van de Velde CJH, Frangioni JV, Vahrmeijer AL

[1] Shared first authorship

ABSTRACT

Background

Near-infrared (NIR) fluorescent sentinel lymph node (SLN) mapping in breast cancer requires optimized imaging systems and lymphatic tracers.

Methods

A small, portable version of the FLARE™ imaging system, termed Mini-FLARE™, was developed for capturing color video and two semi-independent channels of NIR fluorescence (700 nm and 800 nm) in real-time. Initial optimization of lymphatic tracer dose was performed using 35-kg Yorkshire pigs and a 6-patient pilot clinical trial. More refined optimization was performed in twenty-four consecutive breast cancer patients. All patients received the standard of care using [99m]Technetium-nanocolloid and patent blue. In addition, 1.6 mL of indocyanine green adsorbed to human serum albumin (ICG:HSA) was injected directly after patent blue at the same location. Patients were allocated to one of eight escalating ICG:HSA concentration groups from 50 to 1000 μM.

Results

The Mini-FLARE™ system was positioned easily in the operating room and could be used up to 13" from the patient. Mini-FLARE™ enabled visualization of lymphatic channels and SLNs in all patients. A total of 35 SLNs (mean = 1.45, range 1-3) were detected: 35 radioactive (100%), 30 blue (86%), and 35 NIR fluorescent (100%). Contrast agent quenching at the injection site and dilution within lymphatic channels were major contributors to signal strength of the SLN. Optimal injection dose of ICG:HSA ranged between 400 and 800 μM. No adverse reactions were observed.

Conclusions

We describe the clinical translation of a new NIR fluorescence imaging system and define the optimal ICG:HSA dose range for SLN mapping in breast cancer.

INTRODUCTION

Sentinel lymph node (SLN) mapping, as introduced for the management of breast cancer by Giuliano et al,[1] is currently regarded as the standard of care for staging of the axilla.[2] In general, a combination of radioactive colloid and blue dye is used. However, this exposes patients and caregivers to ionizing radiation, and blue dyes cannot be seen through skin and fatty tissue. Nonetheless, in recent trials, SLN identification rates of 95-97% are achieved when using this combination, and use of only one agent results in significantly lower identification rates.[3-6]

Recent preclinical and clinical data have demonstrated that near-infrared (NIR) fluorescence imaging using the NIR fluorescence agent indocyanine green (ICG) enables real-time transcutaneous and intraoperative visualization of lymphatic channels and detection of the SLN.[7-14] Therefore, NIR fluorescence imaging could provide an alternative for, or an addition to, conventional techniques used for SLN mapping. However, to date, clinical data are lacking a direct comparison of NIR fluorescence to the combination of radioactive tracer and blue dye. Also, even though ICG is the only fluorescent agent currently available in the clinic, it is not an optimal lymphatic tracer. Previous preclinical work has demonstrated that adsorption of ICG to human serum albumin (HSA, complex is ICG:HSA) increases the fluorescence intensity and the hydrodynamic diameter, thereby providing improved detection and better retention in the SLN.[15]

Recently, first-in-human clinical testing of ICG:HSA was performed.[14] The Fluorescence-Assisted Resection and Exploration (FLARE™) imaging system, developed by our group[14, 16] and used in the trial, is a general-purpose optical imaging platform that provides the surgeon with two independent NIR fluorescence channels (centered at 700 nm and 800 nm) to see otherwise invisible structures within the surgical field. The first generation of FLARE™ was large, expensive to build, and had a heavy imaging head that required a specially-designed articulated arm.[14] This prevented shipment of FLARE™ to researchers around the world, and therefore impeded efficient scientific investigation. During the first-in-human clinical testing of FLARE™, it also became apparent that contrast agents for SLN mapping were not yet optimal. The goals of the present study were to develop a miniaturized version of FLARE™, termed Mini-FLARE™, and to determine optimal lymphatic tracer dosing for SLN mapping in breast cancer.
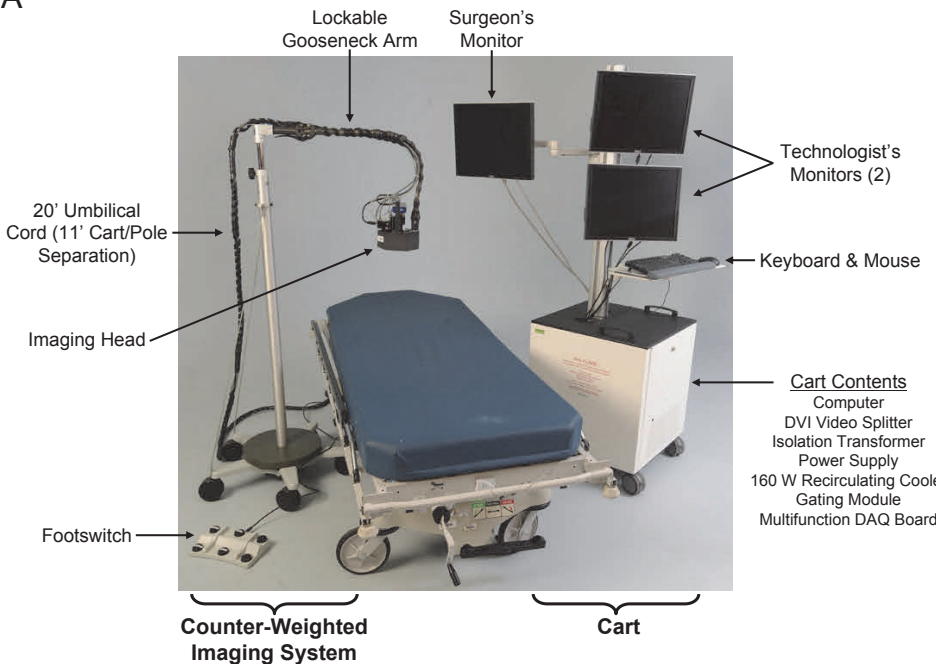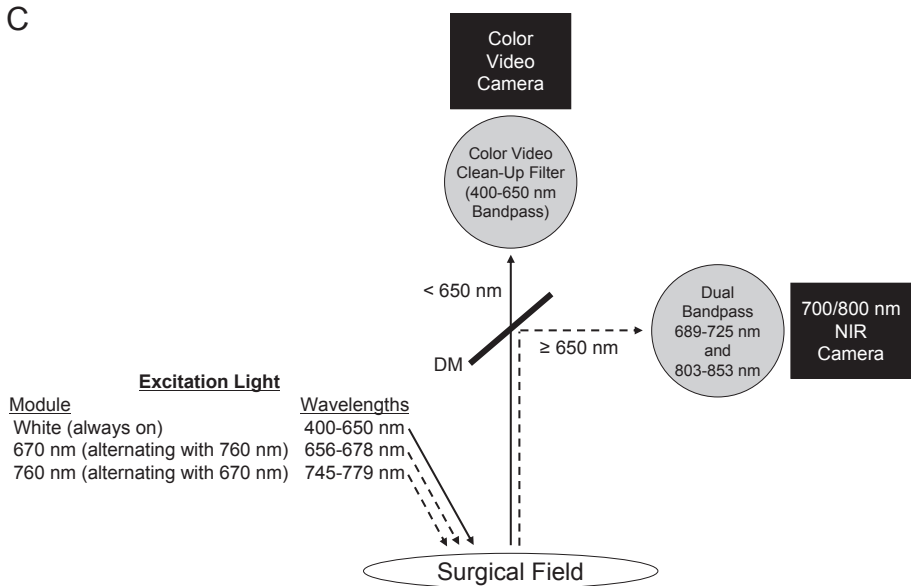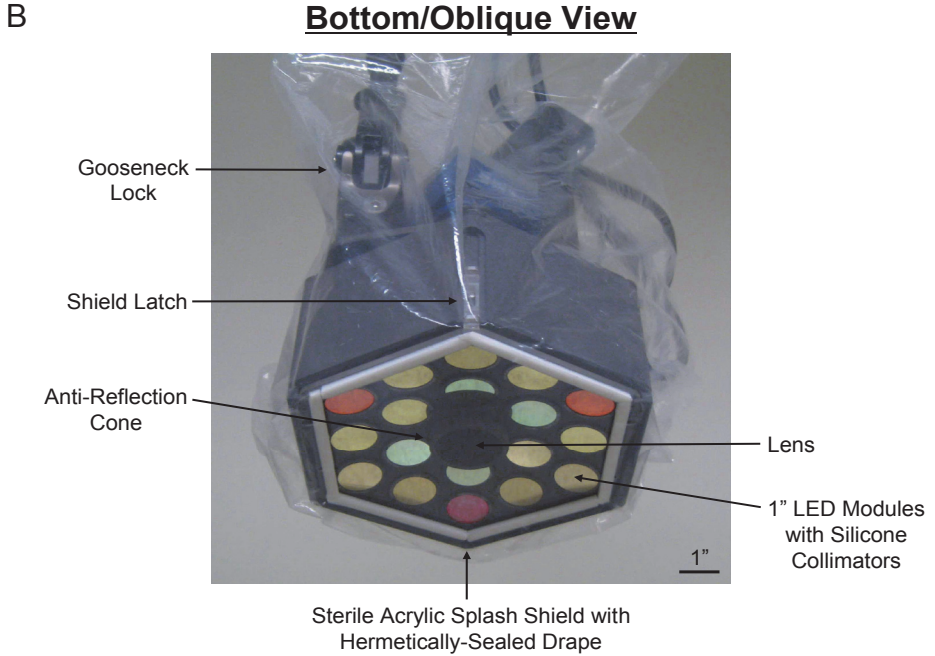
MATERIAL AND METHODS

Mini-FLARE™ imaging system

A detailed description of the Mini-FLARE™ imaging system and *in vitro* characterization is available online at http://www.springerlink.com/content/r4712247933613tv/. For sterile usage in the operating room, a 0.118" thick acrylic splash shield having 95% optical transmission at 800 nm was hermetically bonded to a clear plastic drape and sterilized (Medical Technique, Inc., Tucson, USA).

Preparation of indocyanine green adsorbed to human serum albumin

ICG (25-mg vials) was purchased from Pulsion Medical Systems (Munich, Germany) and was resuspended in 10 cc of sterile water for injection to yield a 2.5 mg/ml (3.2 mM) stock solution. Various amounts of this stock solution were transferred to a 50 cc vial of Cealb (20% human serum albumin (HSA) solution; Sanquin, Amsterdam, The Netherlands) to yield ICG in HSA (ICG:HSA) at a final concentration of 50 μM, 100 μM, 200 μM, 400 μM, 500 μM, 600 μM, 800 μM, or 1000 μM. To obtain a final concentration of 800 μM and 1000 μM, ICG was resuspended in 5 cc of sterile water, to yield a 6.4-mM stock solution prior to dilution.

B

Bottom/Oblique View

Gooseneck Lock

Shield Latch

Anti-Reflection Cone

Lens

1" LED Modules with Silicone Collimators

1"

Sterile Acrylic Splash Shield with Hermetically-Sealed Drape

C

Color Video Camera

Color Video Clean-Up Filter (400-650 nm Bandpass)

< 650 nm

DM

≥ 650 nm

Dual Bandpass 689-725 nm and 803-853 nm

700/800 nm NIR Camera

Excitation Light

Module	Wavelengths
White (always on)	400-650 nm
670 nm (alternating with 760 nm)	656-678 nm
760 nm (alternating with 670 nm)	745-779 nm

Surgical Field

Figure 1. The Mini-FLARE™ portable near-infrared fluorescence imaging system. A. Imaging system composed of electronics/monitor cart and counter-weighted imaging system pole. **B.** Sterile drape/shield attached to the imaging head with other major parts identified. **C.** Excitation and emission light paths, and filtration for the Mini-FLARE™ imaging system. DM = 650 nm dichroic mirror.

Pre-clinical characterization

Animals were studied under the supervision of approved institutional protocol. Female Yorkshire pigs (E. M. Parsons and Sons, Hadley, USA) averaging 35 kg were induced with 4.4-mg/kg intramuscular Telazol (Fort Dodge Labs, Fort Dodge, USA), intubated, and maintained with 2% isoflurane (Baxter Healthcare, Deerfield, USA). Vital signs were monitored continuously. Excitation fluence rate for white light and 800-nm excitation light were 26,600 lux and 7.7 mW/cm^2, respectively. One hundred microliters of the specified ICG:HSA solution was injected intradermally. ICG concentration of the ICG:HSA complex was systematically increased from 10 μM to 500 μM to explore the counteracting effects of NIR fluorophore quenching at the injection site and NIR fluorophore dilution within the lymphatic channels.

Dose-optimization clinical trial

A 24-patient dose-escalation clinical trial was approved by the Medical Ethics Committee of the Leiden University Medical Center and was performed in accordance with the ethical standards of the Helsinki Declaration of 1975. All patients that had planned to undergo a SLN procedure for invasive breast cancer or extensive high-risk carcinoma *in situ* were eligible for participation in the study. Patients had clinically negative axillary nodes as assessed by palpation and ultrasonography. Exclusion criteria were pregnancy, lactation or an allergy to iodine, shellfish, or indocyanine green.

Twenty-four consecutive patients were included. All patients gave informed consent and were anonymized. Patients received the standard-of-care SLN procedure. For our institution, this implies one periareolar injection of approximately 100 MBq ^{99m}Technetium-nanocolloid (mean ± S.D. = 99.6 ± 5.8 MBq) the day before surgery. Before the start of the operation, one mL of patent blue V was injected peritumorally or periareolarly. Choice of the injection site was left to the surgeon. Directly after patent blue injection, 1.6-mL ICG:HSA was administered as four injections at the same location as the patent blue injections. After surgical scrub and sterile covering of the operation field, NIR fluorescence imaging was performed with the imaging head of the Mini-FLARE™ at approximately 30 cm distance to the surgical field.

The surgical technique consisted of percutaneous assessment of NIR fluorescent signal in the breast and the axilla prior to skin incision. The location and length of the axillary skin incision was determined by the surgeon. Assessment of the surgical field using NIR fluorescence was applied continuously throughout the SLN procedure and surgical exploration. If the SLN was not easily detected by NIR fluorescence, the gamma probe was used to provide direction for surgical exploration. Camera exposure was between 5 to 250 msec as indicated. A SLN exhibiting a signal-to-background ratio (SBR) ≥ 1.1 *in situ* was considered positive by NIR fluorescence. Background

was chosen as an area within the surgical field, directly adjacent (within 1-2 cm) to the SLN.

Routine histopathological frozen analysis of SLNs was performed during surgery. If the patient participated in the After Mapping of the Axilla Radiotherapy or Surgery (AMAROS) trial and was randomized to the radiotherapy arm, no intraoperative frozen analysis was performed. SLNs were fixed in formalin and embedded in paraffin for routine hematoxylin, eosin, and immunohistopathological staining for AE1/AE3 at three levels, with an interval of 150-250 μm, according to the Dutch guidelines for SLN analysis. Patients underwent an axillary lymph node dissection if the SLN was found to contain metastases, except for those patients who participated in the radiotherapy arm of the AMAROS trial. If isolated tumor cells (ITCs) were found (< 0.2 mm), no axillary lymph node dissection was performed.

Table 1. Mini-FLARE™ imaging system specifications

Category	Specification	Description
Physical	Size	Mobile Cart: 24" W x 24" D x 29" H; Mast Height: 76.5"
	Weights	Cart: 272 lbs, including all electronics Arm: 95 lbs, including, stand, gooseneck, and imaging head Imaging Head: 8.8 lbs.
	Arm and Stand	Flexible Arm; Reach: 27" – 64" from floor, 42" from center of stand. Center of stand up to 11 linear feet from cart
Electrical	Voltage and Plug	120 V AC, 60 Hz; single NEMA 5-15 120 V/15 A AC plug
	Current	5 A max
	Grounding	Isolation transformer for all components; redundant chassis grounding
	Leakage Current	< 300 μA (per AAMI/IEC #60601)
Sterility	Shield	Disposable acrylic shield with ≥95% transmission
	Drape	Disposable, custom-fit plastic drape bonded to shield
Light Source	Housing	Anodized aluminum with integrated liquid cooling
	Elements	Custom 25 mm circular LED arrays w/ integrated linear drivers
	Electronics	Custom control board with embedded microcontroller
	Fluence Rates	26,600 lux white light (400-650 nm), 1.08 mW/cm^2 of 700 nm (656-678 nm) excitation light, 7.70 mW/cm^2 of 800 nm (745-779 nm) excitation light
Optics	Working Distance	4" (10 cm) to 13" (32 cm) from patient (reverse telephoto)
	Field-of-View	12 cm W x 9 cm H at 13" working distance
	Emission/Reflectance Channels	Color Video (400-650 nm), 700 nm fluorescence (689-725 nm), 800 nm fluorescence (800-848 nm), all with simultaneous acquisition
	Pixel Resolution	640 x 480 for each camera
	System Resolution	320 x 320 μm (x,y)
	Display Refresh	Up to 15 Hz simultaneous acquisition on both cameras
	NIR Exposure Time	Adjustable from 100 μsec to 8 sec
Hands-Free	Optics	Automatic focus
	Control	6-pedal footswitch
Monitors	Number	3 cart-mounted 20": 2 for operator and 1 for surgeon

Statistical analysis

For statistical analysis, SPSS statistical software package (Version 16.0, Chicago, USA) was used. Graphs were generated using GraphPad Prism Software (Version 5.01, La Jolla, USA). To compare the SBR between concentration groups, a one-way analysis of variance (ANOVA) was performed with pairwise comparison with least square difference (LSD) adjustment for multiple testing. When the assumption of homogeneity of variance was violated (Levene's test), a log10 transformation was applied. All statistical tests were two-tailed and $P < .05$ was considered significant.

RESULTS

Design of the Mini-FLARE™ imaging system and *in vitro* characterization

The Mini-FLARE™ imaging system (Figure 1A) is composed of a small portable electronics cart and a counter-weighted pole stand that supports the imaging head. Unlike FLARE™, Mini-FLARE™ utilizes a flexible gooseneck arm, which permits positioning of the imaging head at extreme angles virtually anywhere over the surgical field. The only consumable for Mini-FLARE™ is a specially designed acrylic splash plate that is hermetically sealed to a plastic drape. Using sterile technique, the shield/drape is inserted into the imaging head, locked into place, and the drape is unfolded to encase the imaging head and imaging system pole stand (Figure 1B). Optical light paths for white light (i.e., color video images) and the two semi-independent NIR fluorescence channels, one centered at 700 nm emission and the other at 800 nm emission, are shown in Figure 1C.

Technical specifications of Mini-FLARE™ are detailed in Table 1. Of note, the working distance is up to 13" away from the patient, with field-of-view adjustable from 4.7" (12 cm) to 2" (5 cm) simply by moving the device toward or away from the surgical field. The cart occupies a volume of only 9.7 cu ft, and weighs only 272 lbs. A 6-pedal footswitch and autofocus circuit permit hands-free operation. The cost of all parts is ≈ $40,000.
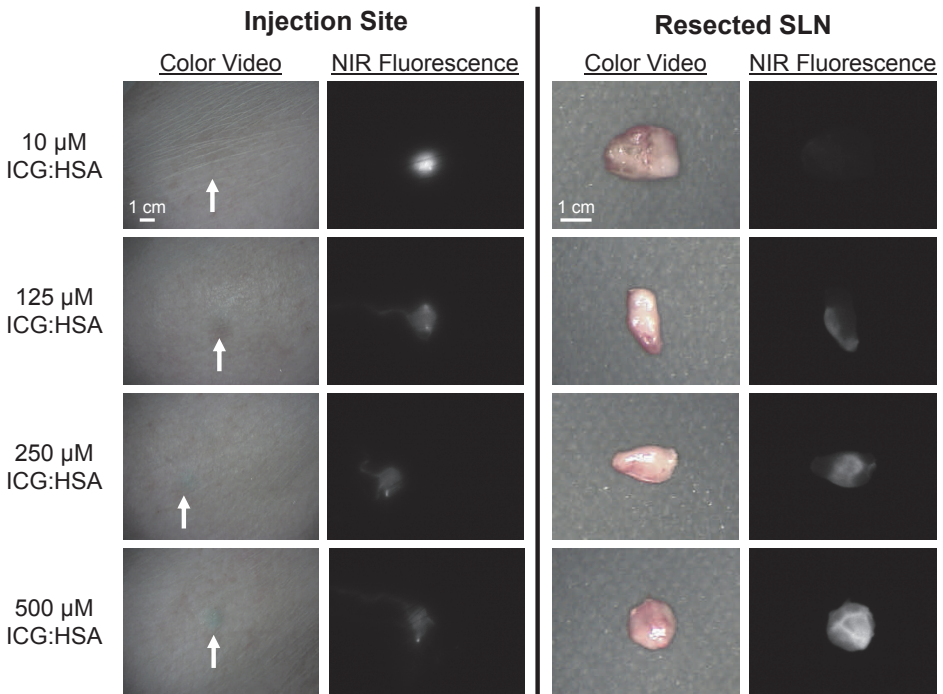
Pre-clinical optimization of NIR fluorescent lymphatic tracers

Our group has previously reported that ICG (and ICG:HSA) exhibits intense quenching (i.e., reduction of fluorescence emission) as its concentration is increased.[15] That is, increasing concentration actually decreases fluorescence, so there would theoretically be no benefit to injecting high concentration for SLN mapping. This effect is demonstrated vividly in Figure 2 (left panel), where the injection site becomes dramatically less fluorescent as concentration increases. As a general rule, if the

concentration is high enough to see green color at the injection site, ICG fluorescence is severely quenched.

Importantly, we have recently discovered that dilution of the injected NIR fluorophore as it travels through the lymphatic system and mixes with lymph counteracts the effect of quenching and results in signal in the SLN that increases with concentration, even when the injection site is barely fluorescent (Figure 2, right panel). This suggests that there will be an "optimal" concentration of injected NIR fluorophore such that final signal in the SLN is as high as possible.

In Vivo Dilution of Lymphatic Tracers

Figure 2. Optimization of ICG:HSA dose as a function of the complex tradeoff between fluorescence quenching at the injection site and dilution of fluorophore in lymphatic channels. Pre-clinical studies in Yorkshire pigs. Subcutaneous injection sites (left; white arrows) showing quenching and resected SLNs (right) showing NIR fluorophore dilution for increasing concentrations of ICG:HSA. For each are displayed color video (left columns) and 800 nm NIR fluorescence (right columns) images obtained using 760 nm excitation light at 7.7 mW/cm². All camera exposure times were 45 msec. Data are representative of N = 3 pigs.

Optimization of ICG:HSA dose in breast cancer patients undergoing SLN mapping

This study aimed to test the feasibility of NIR fluorescence in SLN detection, using ICG:HSA and the Mini-FLARE™, in direct comparison with the conventional lymphatic tracers radiocolloid and patent blue. Twenty-four consecutive breast cancer

patients underwent standard-of-care SLN mapping with the addition of preoperative ICG:HSA injection and subsequent intraoperative NIR fluorescence imaging. Patient and tumor characteristics are provided in Table 2. Use of the Mini-FLARE™ during surgery did not interfere with the standard of care. Average time between ICG:HSA injection and skin incision was 16 ± 3 minutes (Table 3). In all patients (N = 24), NIR fluorescence imaging enabled visualization of the SLN (Figure 3). A total of 35 SLNs were identified, which were all radioactive and NIR fluorescent (Table 3). Five SLNs from four patients did not have blue staining from patent blue. In all patients, the NIR fluorescence signal in the SLN was detected before patent blue. Average time between skin incision and resection of the first SLN was 17 ± 5 minutes. After resection of all nodes detected using NIR fluorescence, the axilla was systematically inspected for any remaining radioactivity. No additional radioactive nodes were identified that were not detected by NIR fluorescence. No adverse reactions associated with the use of ICG:HSA or the Mini-FLARE™ occurred. Two patients experienced a wound infection requiring antibiotics and one patient underwent surgical re-exploration because of an expanding hematoma following axillary lymph node dissection (Table 3).

A second objective of this trial was to determine the optimal concentration of injected ICG:HSA for NIR fluorescence SLN mapping, i.e. which concentration provides the highest SBR in the SLN. Because ICG and ICG:HSA exhibit intense quenching as their concentrations are increased (typically above 50 μM), there would be theoretically no advantage of injecting higher doses of ICG:HSA. However, dilution of the lymphatic tracer occurs upon injection in the breast and uptake by the lymphatic system counteracting the quenching effect. To assess the relationship between the
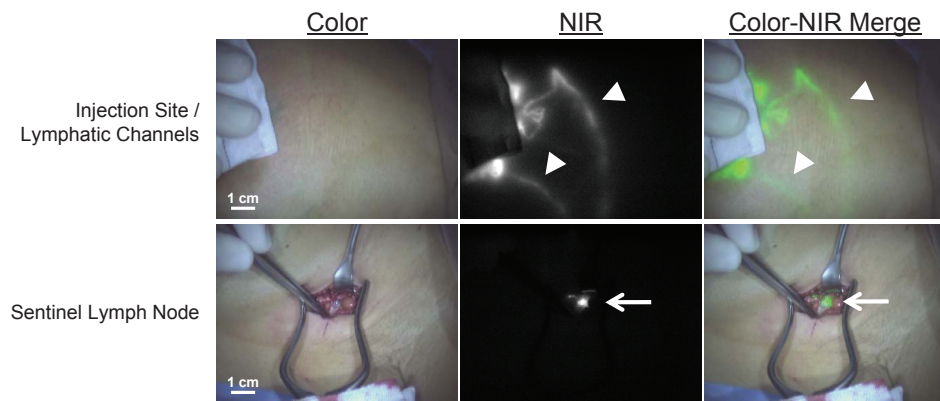
Figure 3. Real-time NIR fluorescence imaging during sentinel lymph node mapping in women with breast cancer. Shown are typical intraoperative results from a subject injected with 600 μM ICG:HSA demonstrating visualization of lymphatic channels (white arrowhead) of the breast running into the axilla from the partially covered periareolar injection site (top row) and detection of the sentinel lymph node (white arrow) in the axilla (bottom row). Camera exposure times were 67 msec (top row) and 20 msec (bottom row). 760 nm excitation fluence rate was ≈ 7.7 mW/cm^2 for all images.

concentration of injected NIR fluorescent lymphatic tracer and final SBR in the SLN, patients were allocated to eight ICG:HSA concentration groups ranging from 50 μM to 1000 μM. The concentration of ICG:HSA influenced the SBR and showed a normal distribution (Figure 4). The variances of the concentration groups were not equal (Levene's test, $P = .02$). A log10 transformation of the data could account for part of the unequal variances (Levene's test, $P = .05$). A one-way ANOVA with pairwise

Table 2. Patient and tumor characteristics

Characteristic	N	%
Age (median, range)	59.5 (33-81)	
Menopausal state		
- Premenopausal	5	21
- Postmenopausal	19	79
Body Mass Index (median, range)	25 (18-38)	
Skin type		
- II	4	17
- III	20	83
Previous breast surgery [a]	3	13
Multifocality	4	17
Tumor side		
- Left	14	58
- Right	10	42
Tumor localization		
- Central	5	21
- Lower inner	1	4
- Lower outer	1	4
- Upper inner	6	25
- Upper outer	11	46
Type of operation		
- Ablation	9	38
- Wide Local Excision	15	63
Pathological tumor size (median, range)	15 (3-35)	
Histological type		
- Infiltrating ductal adenocarcinoma	18	75
- Infiltrating lobular adenocarcinoma	2	8
- Ductal carcinoma *in situ*	4	17
Histological grade		
- I	3	13
- II	13	54
- III	8	33
Receptor status [b]		
- ER+ HER2-	16	67
- ER+ HER2+	3	13
- ER- HER2-	1	4
- Missing [c]	4	17

[a] Previous breast surgery (N = 3): silicone breast implantation, breast reduction and re-excision.
[b] HER2 status was determined using the chromogenic *in situ* hybridization (CISH) kit of Zymed (Invitrogen, Carlsbad, CA)
[c] Not applicable in four patients with ductal carcinoma *in situ*.

comparison with LSD adjustment for multiple comparison showed that the SBRs of the 400, 500, 600, and 800 µM concentration groups were significantly higher than of the 50, 100, 200, and 1000 µM concentration groups (200 vs. 400, P = .001; 200 vs. 500, P = .001; 200 vs. 600, P < .0001; 200 vs. 800, P = .001; 1000 vs. 400, 500, 600 and 800, all P < .0001). The SBRs of the 400, 500, 600, and 800 µM concentration groups were not significantly different, although a trend was found favoring the 600 µM concentration group (500 vs. 600, P = .06). The decline of the SBR in the 1000 µM concentration group was caused by decreased NIR fluorescence signal of the SLN (800 vs. 1000, P = .001), which suggests that quenching of ICG indeed occurred in the SLN.
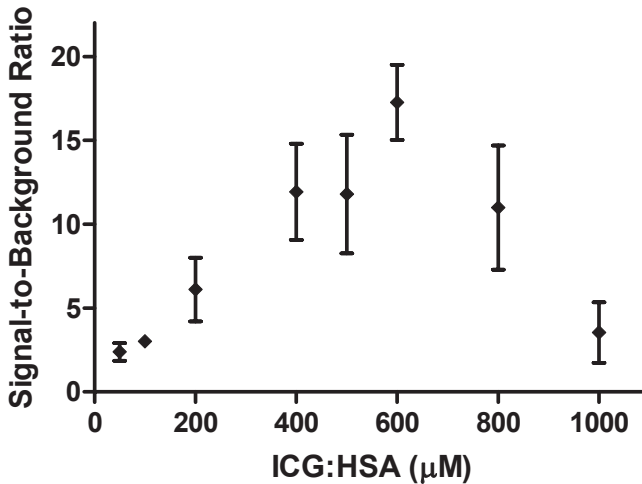
Figure 4. Optimization of ICG:HSA concentration for breast cancer SLN mapping. Signal-to-background ratio (mean ± S.D.) of the SLNs (ordinate) as a function of injected concentration of ICG:HSA (abscissa) in women undergoing SLN mapping for breast cancer. Statistical comparisons are as follows: 200 µM vs. 400 µM, P = .001; 200 µM vs. 500 µM, P = .001; 200 µM vs. 600 µM, P < .0001; 200 µM vs. 800 µM, P = .001; 1000 µM vs. 400, 500, 600 and 800 µM, all P < .0001. The SBRs of the 400, 500, 600 and 800 µM concentration groups were not significantly different, although a trend was found favoring the 600 µM concentration group (500 vs. 600, P = .06).

DISCUSSION

Near-infrared (NIR) fluorescent light in the wavelength range of 700 to 900 nm is invisible to the human eye. It is also capable of penetrating millimeters into living tissue and is not obscured by autofluorescence. For these reasons, NIR fluorescent light is ideal for image-guided surgery. Indeed, several NIR fluorescence surgical imaging systems are already FDA-approved or are in the process of obtaining approval (reviewed in [17]). The Mini-FLARE™ camera system used in this study is capable of displaying NIR fluorescence signal in relation to the surgical anatomy and illuminates the surgical field with white light. This enabled the surgeon to perform surgery under direct image guidance.

NIR fluorescence optical imaging using Mini-FLARE™ offers the advantages of real-time, continuous, high-resolution, and high sensitivity detection of SLNs, without the need for ionizing radiation. Because NIR light is invisible, there is no staining of the surgical field as with blue dyes, and the class of chemicals in which ICG belongs has a remarkable safety record in humans. ICG:HSA adds approximately $150 to the cost of a case, but if future studies show that the blue dye and/or Tc-99m sulfur colloid can be eliminated when using NIR fluorescence, a much larger savings will offset this cost. And, the surgeon can perform the injection procedure only minutes before SLN identification and resection. Although a technologist was used in this first-in-human study, Mini-FLARE™ is equipped with hand-free operation and there is virtually no learning curve because unlike other SLN techniques, the lymphatic tracer can be visualized in real-time throughout the procedure.

Table 3. SLN identification results

Characteristic	N	%
Injection site patent blue and ICG:HSA		
- Periareolar	20	83
- Peritumoral	4	17
SLN detection		
- Number of SLNs identified	35	
- Average number of SLNs identified (range)	1.45 (1-3)	
Method of detection		
- Radioactive	35	100
- Blue	30	86
- Near-infrared fluorescence	35	100
Average time between injection of ICG:HSA and skin incision (S.D.)	16 minutes ± 3	
Average time between skin incision and SLN resection (S.D.)	17 minutes ± 5	
Histology		
- Negative	26	74
- Isolated tumor cells	3	9
- Micrometastases	0	0
- Macrometastases	6	17
Axillary treatment		
- None	16	67
- Axillary lymph node dissection	5	21
- Axillary radiotherapy	3	13
Complications		
- No	21	87
- Yes	3 [a]	13

Abbreviations: ICG:HSA = indocyanine green adsorbed to human serum albumin, SLN = sentinel lymph node, S.D. = standard deviation
[a] Two patients experienced postoperative wound infection requiring treatment with antibiotics and one patient underwent surgical re-exploration because of an expanding hematoma following axillary lymph node dissection.

An important objective of the study was to optimize NIR fluorescent contrast agent dose for breast cancer SLN mapping. The only clinically available NIR fluorescent lymphatic tracer, albeit approved for other indications, is ICG.[7, 11, 13, 18, 19] We have previously proposed simple mixing of ICG and HSA (ICG:HSA) prior to injection[14, 15] because ICG is a small molecule and like blue dyes can pass through SLNs, and exhibit a relatively low quantum yield in aqueous environments.[15] Indeed, the product insert for ICG notes that it rapidly binds albumin when injected intravenously, so pre-mixing merely improves kinetics. Importantly, though, pre-mixing increases quantum yield (i.e., brightness) 3-fold and also results in a final hydrodynamic diameter ($\approx$ 7 nm) that is better retained in the SLN.[15]

NIR fluorescent signal in the SLN is a complex function of the concentration of the injected NIR lymphatic tracer, the distance between the injection site and the SLN, the volume of ultra-filtrate within the lymphatic channels encountered by the NIR fluorophore, and retention of the NIR fluorophore by the SLN. Of these, only the injection concentration can be controlled. Our study suggested that an optimal ICG:HSA concentration is in the range 400 μM and 800 μM. In the 1000 μM concentration group, the fluorescence intensity of the SLN and the SBR decreased rapidly, most likely due to quenching. Furthermore, since lymphatic vessels could be visualized percutaneously and directly after incision, particularly in the optimal dose range groups, a more efficient identification of SLNs was facilitated. This is of particular benefit for lymph nodes located deeper in the axilla, which exceed the 1-2 cm depth limit of the technology. These nodes could often be located by following the NIR fluorescent signal of the afferent lymphatic tract.

The accuracy of SLN identification using ICG fluorescence was similar to that using conventional radioisotope scanning, as both techniques identified all SLNs and no additional fluorescent lymph nodes were identified. However, blue dye identification was not successful in 5 of 35 (14%) SLNs. These results suggest that patent blue staining can be replaced by NIR fluorescence using ICG:HSA. Replacing patent blue has the additional advantage of absent tattooing of the breast and visual alteration of the surgical field. Moreover, the intrinsic dark color of patent blue dye can obscure the fluorescence intensity of any fluorescent lymphatic tracer. Indeed, *in vitro* tests using a fixed ICG:HSA concentration showed that addition of patent blue dye decreased NIR fluorescence of ICG:HSA (data not shown). An as yet unanswered question is whether radioisotope scanning can be omitted from the SLN procedure. A larger trial to address whether NIR fluorescence imaging alone can replace blue dyes and/or radiocolloids is ongoing.

In summary, this study demonstrated feasibility and accuracy of NIR fluorescence imaging using ICG:HSA and the Mini-FLARE™ imaging system for SLN mapping in breast cancer patients. The optimal dose of injected ICG:HSA lies between 400 μM and 800 μM and can be chosen based on local preparation preferences. For example, in the United States, a dose of 500 μM is most convenient since it requires minimal manipulation of albumin volumes.

ACKNOWLEDGEMENTS

REFERENCES

1. Giuliano AE, Kirgan DM, Guenther JM, et al. Lymphatic mapping and sentinel lymphadenectomy for breast cancer. Ann Surg 1994; 220:391-8.
2. Cox CE, Pendas S, Cox JM, et al. Guidelines for sentinel node biopsy and lymphatic mapping of patients with breast cancer. Ann Surg 1998; 227:645-51.
3. Goyal A, Newcombe RG, Chhabra A, et al. Factors affecting failed localisation and false-negative rates of sentinel node biopsy in breast cancer - results of the ALMANAC validation phase. Breast Cancer Res Treat 2006; 99:203-8.
4. Krag DN, Anderson SJ, Julian TB, et al. Technical outcomes of sentinel-lymph-node resection and conventional axillary-lymph-node dissection in patients with clinically node-negative breast cancer: results from the NSABP B-32 randomised phase III trial. Lancet Oncol 2007; 8:881-8.
5. Straver ME, Meijnen P, van Tienhoven G, et al. Sentinel node identification rate and nodal involvement in the EORTC 10981-22023 AMAROS trial. Ann Surg Oncol 2010; 17:1854-61.
6. Zavagno G, De Salvo GL, Scalco G, et al. A Randomized clinical trial on sentinel lymph node biopsy versus axillary lymph node dissection in breast cancer: results of the Sentinella/GIVOM trial. Ann Surg 2008; 247:207-13.
7. Hirche C, Murawa D, Mohr Z, et al. ICG fluorescence-guided sentinel node biopsy for axillary nodal staging in breast cancer. Breast Cancer Res Treat 2010; 121:373-8.
8. Hojo T, Nagao T, Kikuyama M, et al. Evaluation of sentinel node biopsy by combined fluorescent and dye method and lymph flow for breast cancer. Breast 2010; 19:210-3.
9. Kitai T, Inomoto T, Miwa M, et al. Fluorescence navigation with indocyanine green for detecting sentinel lymph nodes in breast cancer. Breast Cancer 2005; 12:211-5.
10. Murawa D, Hirche C, Dresel S, et al. Sentinel lymph node biopsy in breast cancer guided by indocyanine green fluorescence. Br J Surg 2009; 96:1289-94.
11. Sevick-Muraca EM, Sharma R, Rasmussen JC, et al. Imaging of lymph flow in breast cancer patients after microdose administration of a near-infrared fluorophore: feasibility study. Radiology 2008; 246:734-41.
12. Tagaya N, Yamazaki R, Nakagawa A, et al. Intraoperative identification of sentinel lymph nodes by near-infrared fluorescence imaging in patients with breast cancer. Am J Surg 2008; 195:850-3.
13. Tanaka E, Chen FY, Flaumenhaft R, et al. Real-time assessment of cardiac perfusion, coronary angiography, and acute intravascular thrombi using dual-channel near-infrared fluorescence imaging. J Thorac Cardiovasc Surg 2009; 138:133-40.
14. Troyan SL, Kianzad V, Gibbs-Strauss SL, et al. The FLARE intraoperative near-infrared fluorescence imaging system: a first-in-human clinical trial in breast cancer sentinel lymph node mapping. Ann Surg Oncol 2009; 16:2943-52.
15. Ohnishi S, Lomnes SJ, Laurence RG, et al. Organic alternatives to quantum dots for intraoperative near-infrared fluorescent sentinel lymph node mapping. Mol Imaging 2005; 4:172-81.
16. Gioux S, Kianzad V, Ciocan R, et al. High-power, computer-controlled, light-emitting diode-based light sources for fluorescence imaging and image-guided surgery. Mol Imaging 2009; 8:156-65.
17. Gioux S, Choi HS, Frangioni JV. Image-guided surgery using invisible near-infrared light: fundamentals of clinical translation. Mol Imaging 2010; 9:237-55.
18. Kusano M, Tajima Y, Yamazaki K, et al. Sentinel node mapping guided by indocyanine green fluorescence imaging: a new method for sentinel node navigation surgery in gastrointestinal cancer. Dig Surg 2008; 25:103-8.
19. Yamashita S, Tokuishi K, Anami K, et al. Video-assisted thoracoscopic indocyanine green fluorescence imaging system shows sentinel lymph nodes in non-small-cell lung cancer. J Thorac Cardiovasc Surg 2011; 141:141-4.